Synthesis and Detailed Photophysical Studies of Pyrene−Based Molecules Substituted with Extended Chains

ARTICLE *in* THE JOURNAL OF PHYSICAL CHEMISTRY A · FEBRUARY 2009

Impact Factor: 2.69 · DOI: 10.1021/jp809830x · Source: PubMed

4 AUTHORS, INCLUDING:

Digambara Patra
American University of Beirut
68 PUBLICATIONS **1,497** CITATIONS
SEE PROFILE

Bilal R Kaafarani
American University of Beirut
55 PUBLICATIONS **969** CITATIONS
SEE PROFILE

THE JOURNAL OF PHYSICAL CHEMISTRY A

Article

Synthesis and Detailed Photophysical Studies of Pyrene-Based Molecules Substituted with Extended Chains

Rasha M. Moustafa, Jad A. Degheili, Digambara Patra, and Bilal R. Kaafarani

J. Phys. Chem. A, **2009**, 113 (7), 1235-1243• Publication Date (Web): 20 January 2009

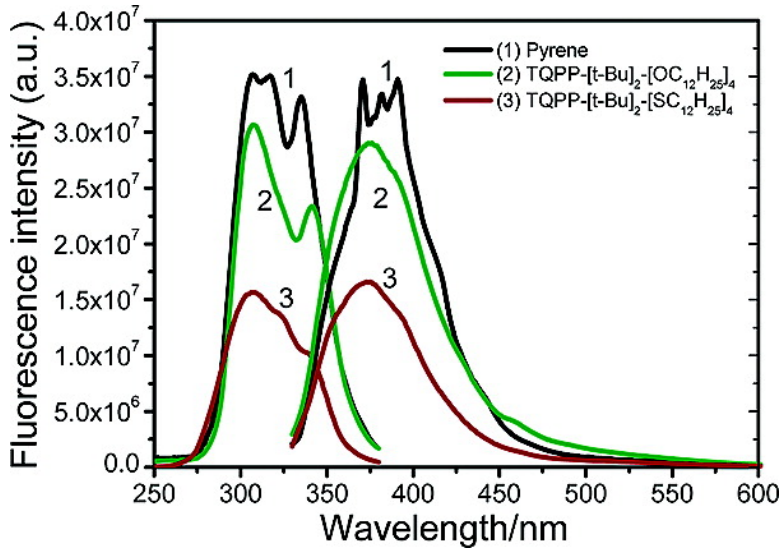

More About This Article

Additional resources and features associated with this article are available within the HTML version:

- Supporting Information
- Access to high resolution figures
- Links to articles and content related to this article
- Copyright permission to reproduce figures and/or text from this article

View the Full Text HTML

The Journal of Physical Chemistry A is published by the American Chemical Society. 1155 Sixteenth Street N.W., Washington, DC 20036

Synthesis and Detailed Photophysical Studies of Pyrene-Based Molecules Substituted with Extended Chains

Rasha M. Moustafa, Jad A. Degheili, Digambara Patra,* and Bilal R. Kaafarani*

Department of Chemistry, American University of Beirut, Beirut 1107-2020, Lebanon

Received: August 8, 2008

Applications of conjugated organic compounds in the field of electronics and optoelectronics and of pyrene derivatives as fluorescent probes are well established. The synthesis of the novel pyrene-based 2,11-di-*tert*-butyl-6,7,15,16-tetrakis(alkoxy/alkythio)quinoxaline[2′,3′:9,10]phenanthro[4,5-*abc*]phenazine, TQPP-[*t*-Bu]$_2$-[XR]$_4$ (X = O, S; R = C_nH_{2n+1}), is reported along with an in-depth spectroscopic characterization and evaluation of their photophysical properties. Despite their larger core size, the reported TQPP materials showed similar fluorescence behavior to that of pyrene itself, with no significant shift in their fluorescence peak. The fluorescence spectra showed peaks corresponding to the monomer and to the excimer. Even though these TQPP compounds showed poor solubility in various solvents, their solvatochromism could be investigated in different solvents ranging from polar solvents such as methanol to nonpolar solvents such as cyclohexane; Stokes shifts, fluorescence lifetimes, fluorescence quantum yields, as well as radiative and nonradiative rate constants are determined for four of these TQPP materials in various solvents. Quantum yields were found to be low for these TQPP compounds in solvents such as tetrahydrofuran (THF), whereas they were relatively higher in cyclohexane and dioxane. Monomer to excimer intensity ratio versus gross solvent scale (E_T30) and orientation polarizabilty (Δf) were correlated. Although TQPP-[*t*-Bu]$_2$-[XR]$_4$ displayed similar fluorescent emission and excitation behavior as that of pyrene, a relatively smaller lifetime was observed for these compounds compared to that of pyrene.

1. Introduction

Organic conjugated compounds are widely used in the field of electronics and optoelectronics. Such materials are being exploited for use in organic light-emitting diodes (OLEDs),[1−5] phototransistors,[6,7] organic photovoltaic cells,[7] and organic field-effect transistors (OFETs).[8−11] Molecules that form discotic liquid crystals typically consist of a central aromatic core to which three to eight flexible chains are attached.[12] Such compounds may form efficient $\pi-\pi$ columnar stacks leading to high charge-carrier mobilities.[13] A value as high as 0.5 cm^2 V^{-1} s^{-1} has been reported in liquid-crystalline hexabenzocoronene derivatives.[14] The magnitude of the mobility, and hence its potential to be exploited in electronic devices, depends on the degree of order and $\pi-\pi$ molecular orbital overlap within the columnar stacks.[15,16]

The polarity of solvents plays a key role in determining many characteristics of discotic compounds,[17] including their solubility and their optical behavior.[18] Studies on optical absorption and emission properties have led the way toward solvatochromic probes, that is, molecules whose optical behavior, including absorption, emission, and/or excitation spectral shifts, greatly depends on the dipolar and dielectric properties of the surrounding solvent or other medium.[18] Fluorescent probes have a wide range of applications such as monitoring the degree of polymerization,[19] radiation cure technology,[20] and photocurable coatings.[21] Polycyclic aromatic hydrocarbons (PAHs) have commonly been used as fluorescent probes.[22−32] Among PAHs, pyrene has been widely studied as a local polarity probe,[18,33,34] rendering pyrene and pyrene-based materials as important molecules in the field of photochemistry and photophysics.[35] Such molecules may act as sensitive fluorescent probes that can undergo changes in their spectral properties, which can include quantum-yield values, fluorescence anisotropy, formation of excimers, vibrational structure of pyrene itself, and any external or internal quenching,[35] leading to better knowledge of the surrounding systems.[18] The area of probes has attracted the efforts of organic and physical chemists toward synthesizing and studying more sensitive molecules, including compounds exhibiting more extensive conjugation than pyrene.[36]

In this paper, we report the synthesis of various pyrene-based molecules with extended chain substituents (Scheme 1) and the investigation of their photophysical properties in various solvents. Their photophysical behavior was characterized by measurements of their absorption spectra, emission spectra, fluorescence lifetimes, quantum yields, and radiative as well as nonradiative rate constants. An investigation of the mesophase behavior in these materials is currently ongoing.

2. Experimental Section

Chemicals and solvents were purchased from Acros. Standard grade silica gel (60 Å, 32−63 μm) and silica gel plates (250 μm) were purchased from Sorbent Technologies. Reactions that required anhydrous conditions were carried out under argon in oven-dried glassware. A Bruker spectrometer was used to record the NMR spectra. $CDCl_3$ was the solvent for NMR and chemical shifts relative to tetramethylsilane (TMS) at 0.00 ppm are reported in parts per million (ppm) on the δ scale. The MALDI data were acquired at the Bioanalytical Mass Spectrometry Facility at the Georgia Institute of Technology, Atlanta, GA. Elemental analyses were performed at Atlantic Microlab Inc., Norcross, GA.

* To whom correspondence should be addressed. E-mail: dp03@aub.edu.lb (D.P.); bilal.kaafarani@aub.edu.lb (B.R.K.). Telephone: +961-1-350 000. Fax: +961-1-365217.

10.1021/jp809830x CCC: $40.75
Published on Web 01/20/2009

SCHEME 1: Synthesis of TQPP-[*t*-Bu]$_2$-[XR]$_4$ (1) and (2)

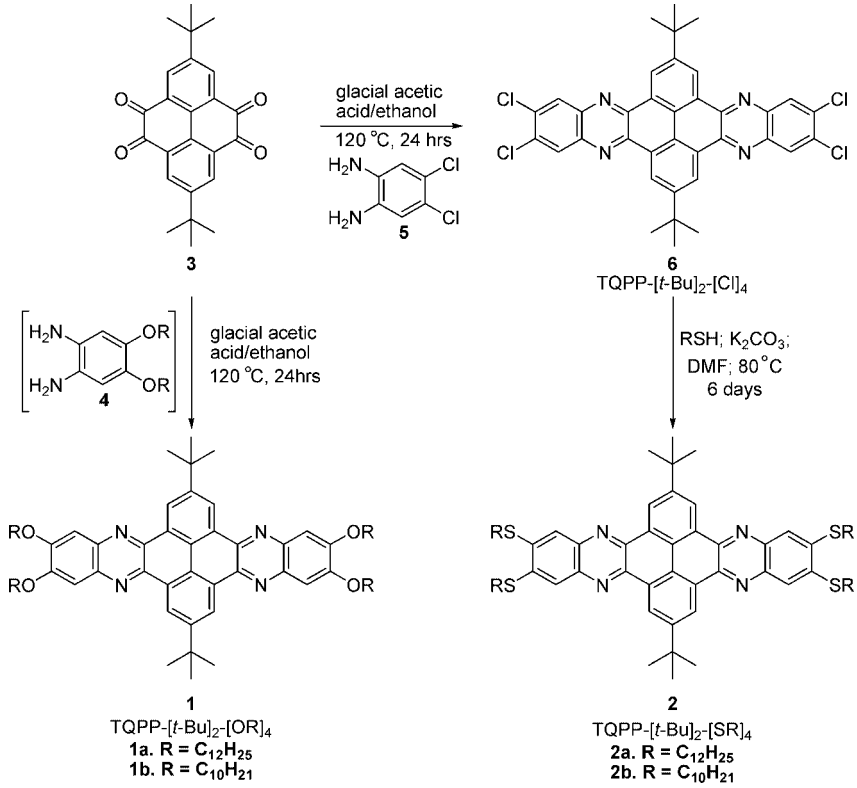

2.1. Synthesis. ***General Procedure for the Synthesis of TQPP-[t-Bu]$_2$-[OR]$_4$ (1a,b).*** The title compound was synthesized according to a modified literature procedure.[37] A solution of (1:1) ethanol/acetic acid (150 mL) was added to a mixture of 2,7-di-*tert*-butylpyrene-4,5-dione (**3**)[38] (1 equiv) and 4,5-di-alkoxy-1,2-phenylenediamine (**4**)[39] (2 equiv). The reaction mixture was refluxed under argon for 24 h. The mixture was cooled on an ice-water bath and was then filtered. The obtained solid was recrystallized from toluene or nitrobenzene, as indicated, purified by column chromatography using chloroform as eluent, and recrystallized again from the indicated solvents.

2,11-Bis(1-methylethyl)-6,7,15,16-tetrakis(dodecyloxy)quinoxaline[2′,3′:9,10]phenanthro[4,5-abc]phenazine, TQPP-[t-Bu]$_2$-[OC$_{12}$H$_{25}$]$_4$ (1a). After column chromatography, the product was recrystallized from toluene to yield yellow solid **1a** (1.21 g, 60%), mp 213−214 °C. ^{1}H NMR (300 MHz, $CDCl_3$, 45 °C): δ 0.89 (12H, t, J = 6.6 Hz), 1.29 (64H, m), 1.60 (8H, quintet, J = 8.9 Hz), 1.76 (18H, s), 2.02 (8H, quintet, J = 7.2 Hz), 4.32 (8H, t, J = 6.6 Hz), 7.61 (4H, s), 9.72 (4H, s). ^{13}C NMR (75.5 MHz, $CDCl_3$): δ 14.15, 22.72, 26.13, 28.97, 29.40, 29.47, 29.68, 29.74, 31.96, 35.89, 69.23, 106.95, 129.56, 139.91, 140.64, 153.24, 166.94. HRMS-MALDI (m/z): [M]$^+$ calcd for $C_{84}H_{126}N_4O_4$, 1254.97; found, 1254.98. Anal. Calcd for $C_{84}H_{126}N_4O_4$: C, 80.33; H, 10.11; N, 4.49. Found: C, 80.05; H, 10.06; N, 4.49.

2,11-Bis(1-methylethyl)-6,7,15,16-tetrakis(decyloxy/alkythio)-quinoxaline[2′,3′:9,10]phenanthro[4,5-abc]phenazine, TQPP-[t-Bu]$_2$-[OC$_{10}$H$_{21}$]$_4$ (1b). After column chromatography, the product was recrystallized from nitrobenzene to yield yellow solid **1b** (1.09 g, 76%), mp 271−273 °C (lit.[37] 267 °C). ^{1}H NMR (300 MHz, $CDCl_3$): δ 0.89 (12H, t, J = 6.62 Hz), 1.25 (48H, m), 1.58 (8H, m), 1.76 (18H, s), 2.03 (8H, quintet, J = 6.93 Hz), 4.33 (8H, t, J = 6.59 Hz), 7.63 (4H, s), 9.72 (4H, s). ^{13}C NMR (75 MHz, $CDCl_3$, 45 °C): δ 14.15, 22.72, 26.12, 28.97, 29.39, 29.46, 29.62, 29.67, 31.95, 35.89, 69.25, 106.98, 122.78, 124.64, 129.58, 139.94, 140.67, 150.26, 153.27. MALDI (m/z): [M]$^+$ calcd for $C_{76}H_{110}N_4O_4$, 1142.8; found, 1142.7. Anal. Calcd for $C_{76}H_{110}N_4O_4$: C, 79.81; H, 9.69; N, 4.90. Found: C, 79.99; H, 9.82; N, 4.86.

General Procedure for the Synthesis of TQPP-[t-Bu]$_2$-[SR]$_4$ (2a,b). TQPP-[*t*-Bu]$_2$-[SR]$_4$ were synthesized according to a modified literature procedure.[40] To a mixture of TQPP-[*t*-Bu]$_2$-[Cl]$_4$ (**6**) (1.00 g, 1.52 mmol) and K_2CO_3 (10.1 g, 73.0 mmol), purged with argon, dimethylformamide (DMF) (100 mL) and alkanethiol (RSH) (24.3 mmol) were added under argon. The reaction mixture was stirred under argon at 80 °C for 6 days. The reaction mixture was poured into H_2O (400 mL), acidified with concentrated HCl to pH = 5, and filtered. The obtained solid was recrystallized from toluene, purified by column chromatography using $CHCl_3$ as eluent, and recrystallized again from toluene.

2,11-Bis(1-methylethyl)-6,7,15,16-tetrakis(dodecanethio)quinoxaline[2′,3′:9,10]phenanthro[4,5-abc]phenazine, TQPP-[t-Bu]$_2$-[SC$_{12}$H$_{25}$]$_4$ (2a). Yellow solid (2.52 g, 72%), mp 272−274 °C. ^{1}H NMR (300 MHz, $CDCl_3$): δ 0.87 (12H, t, J = 6.7 Hz), 1.27 (64H, m), 1.59 (8H, quintet, J = 8.8 Hz), 1.76 (18H, s), 1.92 (8H, quintet, J = 7.5 Hz), 3.28 (8H, t, J = 7.3 Hz), 8.10 (4H, s), 9.73 (4H, s). ^{13}C NMR (75.5 MHz, $CDCl_3$): δ 14.14, 22.71, 28.21, 29.25, 29.33, 29.38, 29.60, 29.67, 29.71, 31.93, 31.97, 33.34, 35.91, 123.90, 125.23, 129.25, 140.56, 141.21, 142.03, 150.49. HRMS-MALDI (m/z): [M]$^+$ calcd for $C_{84}H_{126}N_4S_4$, 1318.886; found, 1318.880. Anal. Calcd for $C_{84}H_{126}N_4S_4$: C, 76.42; H, 9.62; N, 4.24; S, 9.72. Found: C, 76.43; H, 9.69; N, 4.35; S, 9.72.

2,11-Bis(1-methylethyl)-6,7,15,16-tetrakis(decanethio)quinoxaline[2′,3′:9,10]phenanthro[4,5-abc]phenazine, TQPP-[t-Bu]$_2$-[SC$_{10}$H$_{21}$]$_4$ (2b). Yellow solid (1.59 g, 79%), mp 280−282 °C. ^{1}H NMR (300 MHz, $CDCl_3$): δ 0.89 (12H, t, J = 6.9 Hz), 1.29 (48H, m), 1.62 (8H, quintet, J = 6.1 Hz), 1.77 (18H, s), 1.92 (8H, quintet, J = 7.5 Hz), 3.28 (8H, t, J = 7.3 Hz), 8.10

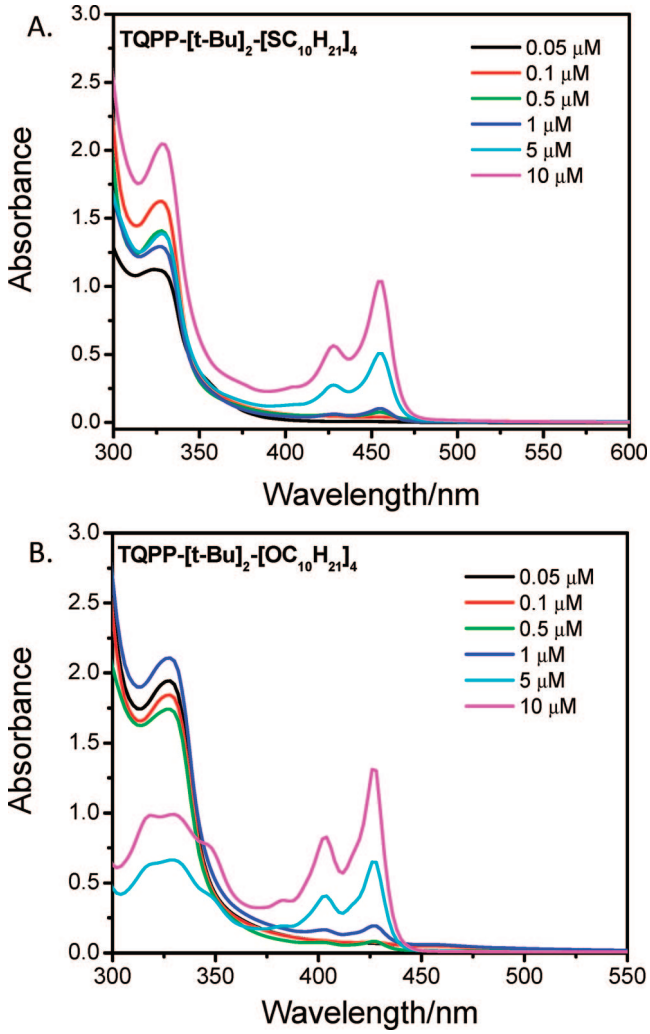

Figure 1. Concentration variation studies for TQPP-[*t*-Bu]$_2$-[XC$_{12}$H$_{21}$]$_4$ in THF by UV−visible absorption spectroscopy.

(4H, s), 9.72 (4H, s). ^{13}C NMR (75.5 MHz, $CDCl_3$): δ 14.13, 22.70, 28.23, 29.21, 29.29, 29.35, 29.57, 29.59, 31.92, 31.93, 33.37, 35.92, 124.01, 125.36, 129.39, 140.68, 141.36, 142.17, 150.65. HRMS-MALDI (*m*/*z*): $[M]^+$ calcd for $C_{76}H_{110}N_4S_4$, 1206.76; found, 1206.73. Anal. Calcd for $C_{76}H_{110}N_4S_4$: C, 75.57; H, 9.18; N, 4.64; S, 10.62. Found: C, 75.72; H, 9.14; N, 4.76; S, 10.63.

2.2. Solution Preparation. Stock solutions of concentration 1 mM were prepared for each compound in tetrahydrofuran (THF). Further dilution was made as required for concentration studies in the range of 50 nM to 10 μM. The solvents used were of spectroscopic grade. Depending upon the solubility of the compounds, six different solvents having different polarities were chosen for the studies, namely, cyclohexane, 1,4-dioxane, THF, 1,2-dichlorobenzene, dichloromethane, and methanol.

2.3. Spectroscopic Measurement. Absorption spectra were measured using a JASCO V-570 UV−vis-NIR spectrophotometer, and the fluorescence measurements were carried out using a Jobin-Yvon-Horiba Fluorolog III spectrofluorimeter. The excitation source is a 100 W xenon lamp, and the detector used is R-928 operating at a voltage of 950 V.

2.4. Fluorescence Lifetime Measurement. The fluorescence lifetime measurements were performed using a Jobin-Yvon-Horiba Fluorolog III spectrofluorimeter, with a pulsed diode laser of excitation wavelength 282 nm. The decay data were analyzed using Data Analysis software. Decay fits with values

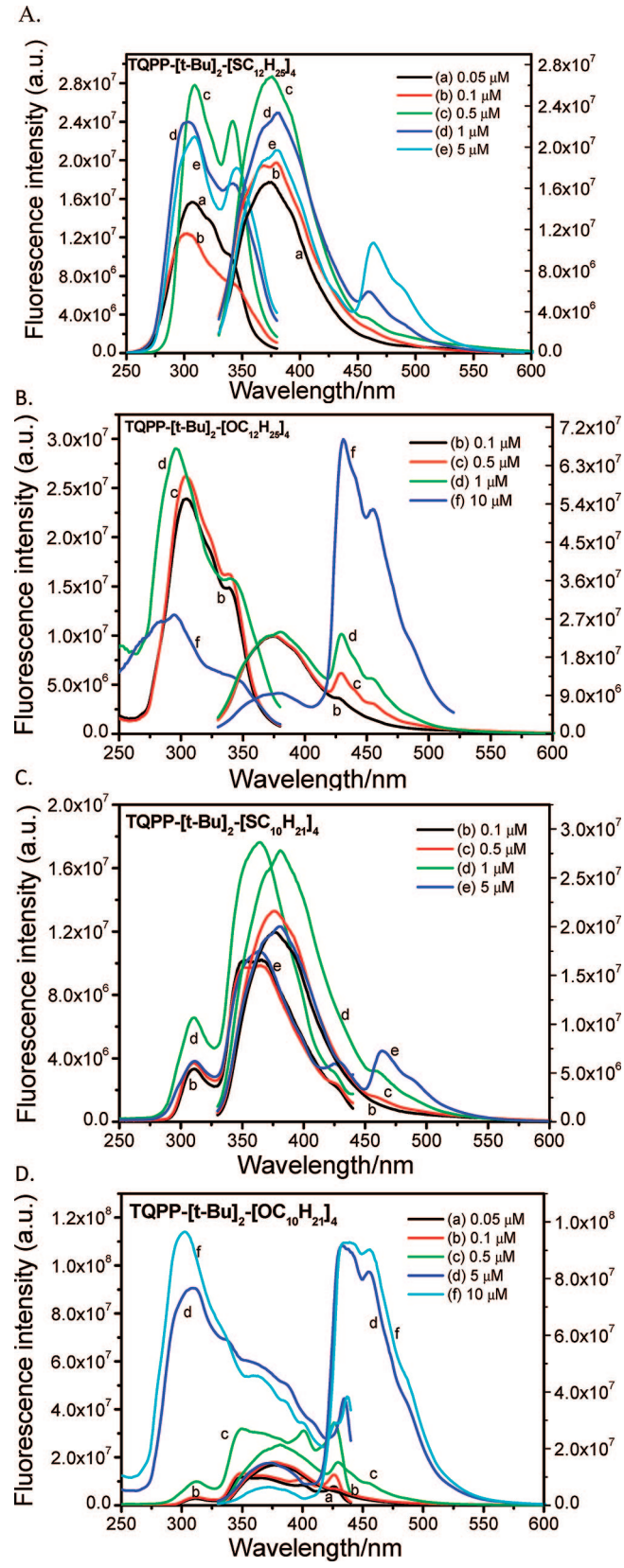

Figure 2. Excitation and emission fluorescence spectra of TQPP-[*t*-Bu]$_2$-[XR]$_4$ in THF at various concentrations.

of χ^2 between 0.99 and 1.5 were considered to be within the acceptable range.

2.5. Determination of the Fluorescence Quantum Yield. For fluorescence quantum yield determination, dilute conditions (concentration range 50−500 nM) were chosen to avoid self-

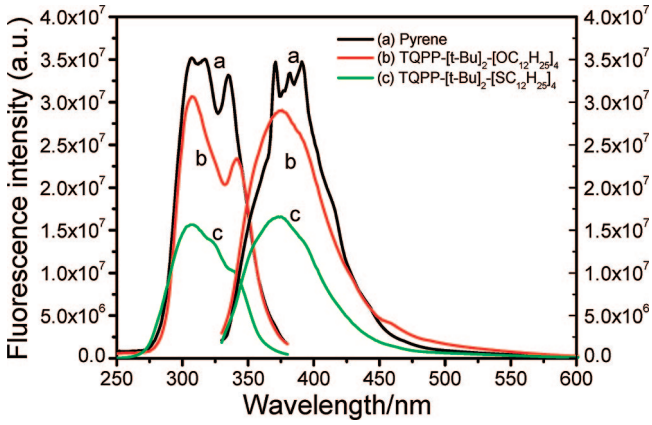

Figure 3. Excitation and emission spectra comparison for pyrene, TQPP-[*t*-Bu]$_2$-[OC$_{12}$H$_{25}$]$_4$, and TQPP-[*t*-Bu]$_2$-[SC$_{12}$H$_{25}$]$_4$ in THF.

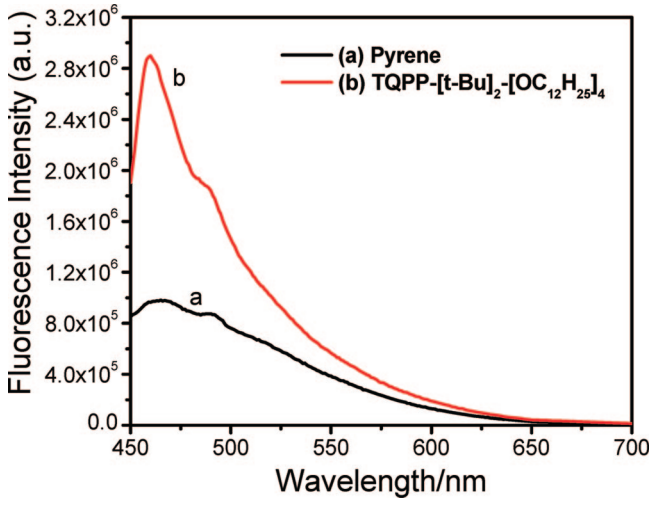

Figure 4. Fluorescence spectra of pyrene and TQPP-[*t*-Bu]$_2$-[OC$_{12}$H$_{25}$]$_4$ at excitation wavelength 390 nm. Both of them show similar excimer emission at this excitation wavelength.

quenching of fluorophores and inner filter effects. Anthracence in ethanol was used as a standard to determine the fluorescence quantum yield of the unknown samples. The excitation wavelength used for the reference and standard sample was 320 nm. The fluorescence quantum yield of TQPP-[*t*-Bu]$_2$-[XR]$_4$ in various solvents was determined using the following equation:[47]

$$\phi_{\mathrm{unk}} = \phi_{\mathrm{std}} \frac{F_{\mathrm{unk}}}{F_{\mathrm{std}}} \frac{A_{\mathrm{std}}}{A_{\mathrm{unk}}} \frac{n_{\mathrm{unk}}^2}{n_{\mathrm{std}}^2}$$

where ϕ_{unk} and ϕ_{Std} are the quantum yield of the sample of interest and that of the reference sample, respectively. The quantum yield of anthracene in ethanol was taken to be 0.31.[42] F_{unk} and F_{std} are the integrated intensities of the emission spectrum of the analyte and that of the reference sample, respectively. *A* corresponds to the optical density of the samples taken at the excitation wavelength (320 nm), and finally, *n* is the refractive index of the solvents used. In the above equation, standard (std) refers to anthracene in ethanol, and unknown (unk) refers to TQPP molecules in the six different solvents.

3. Results and Discussion

The synthesis of TQPP-[*t*-Bu]$_2$-[XR]$_4$ is depicted in Scheme 1. 2,7-Di-*tert*-butylpyrene-4,5-dione (**3**)[38] and 4,5-dialkoxy-1,2-

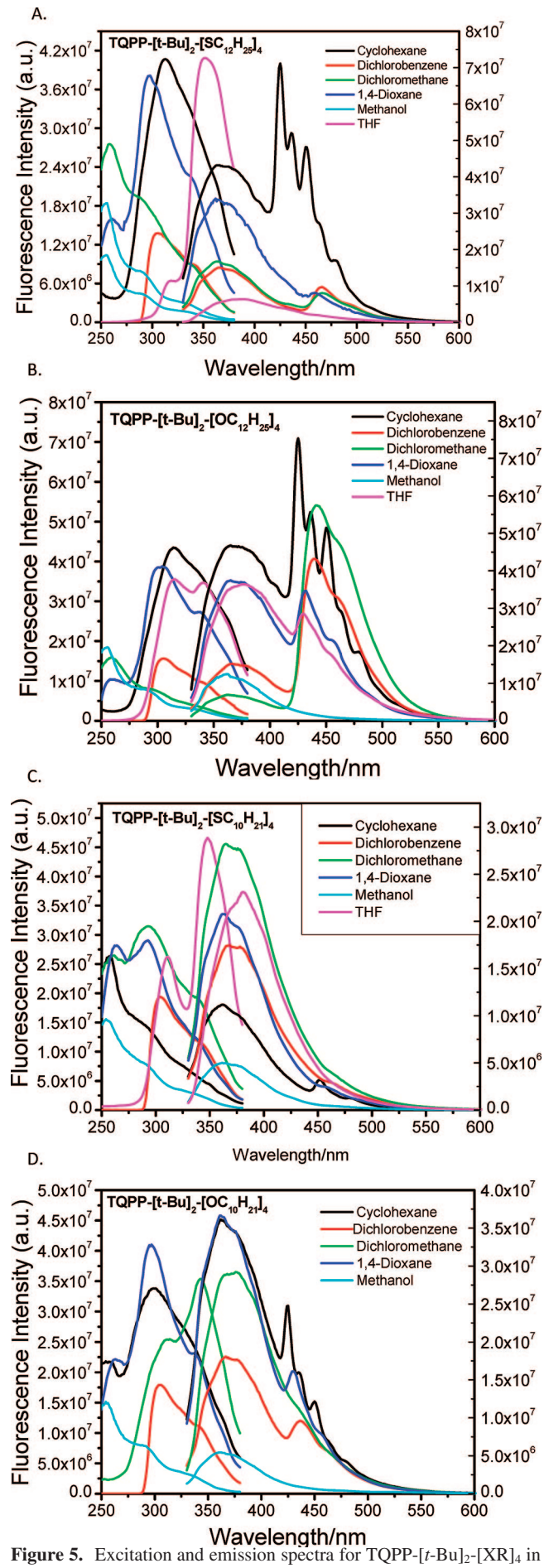

Figure 5. Excitation and emission spectra for TQPP-[*t*-Bu]$_2$-[XR]$_4$ in different solvents.

TABLE 1: Absorption Maxima, Emission Maxima, Stokes Shift, and $I_{monomer}/I_{excimer}$ Ratio for TQPP-[*t*-Bu]$_2$-[XR]$_4$ in Various Solvents[a]

compound	solvents	λ_{abs} (max)/nm	λ_{em} (max)/nm	Stokes shift/cm^{-1}	$I_{monomer}/I_{excimer}$
TQPP-[*t*-Bu]$_2$-[OC$_{12}$H$_{25}$]$_4$	cyclohexane	307	366	5251	2.70
	1,4-dioxane	327	379	4196	3.86
	1,2-dichlorobenzene	328	381	4241	2.54
	THF	329	376	3799	6.06
	dichloromethane	330	376	3707	5.08
	methanol	325	378	4314	5.81
TQPP-[*t*-Bu]$_2$-[SC$_{12}$H$_{25}$]$_4$	cyclohexane	324	362	3230	4.12
	1,4-dioxane	327	363	3033	3.86
	1,2-dichlorobenzene	318	366	4124	5.39
	THF	328	378	4033	6.93
	dichloromethane	330	364	2830	6.70
	methanol	30	360	2525	4.95
TQPP-[*t*-Bu]$_2$-[OC$_{10}$H$_{21}$]$_4$	cyclohexane	320	362	3626	3.13
	1,4-dioxane	327	361	2880	4.37
	1,2-dichlorobenzene	320	367	4002	2.54
	THF	327	380	4265	5.17
	dichloromethane	321	376	4557	3.83
	methanol	327	361	2880	8.91
TQPP-[*t*-Bu]$_2$-[SC$_{10}$H$_{21}$]$_4$	cyclohexane	334	361	2239	3.45
	1,4-dioxane	328	362	2863	8.12
	1,2-dichlorobenzene	322	368	3882	5.02
	THF	326	381	4428	5.17
	dichloromethane	318	365	4049	5.51
	methanol	327	364	3109	9.38

[a] The concentration of fluorophore was 1 μM for absorption and 50 nM for fluorescence measurements.

phenylenediamine (**4**)[39] were heated to reflux in a 1:1 mixture of acetic acid/ethanol to yield TQPP-[*t*-Bu]$_2$-[OR]$_4$ (**1**), whereas condensation of **3** with 3,4-dichloro-1,2-phenylenediamine (**5**) in acetic acid/ethanol (1:1) afforded TQPP-[*t*-Bu]$_2$-[Cl]$_4$ (**6**), which was in turn reacted with alkanethiol to yield TQPP-[*t*-Bu]$_2$-[SR]$_4$ (**2**).

The four TQPP-[*t*-Bu]$_2$-[XR]$_4$ showed two absorptions, with one in the range of 400−460 nm and another at 310−330 nm. Representative concentration-dependent absorption spectra of TQPP-[*t*-Bu]$_2$-[XC$_{10}$H$_{21}$]$_4$ (X = O, S) are depicted in Figure 1. Both TQPP-[*t*-Bu]$_2$-[SC$_{10}$H$_{21}$]$_4$ (Figure 1A) and TQPP-[*t*-Bu]$_2$-[SC$_{12}$H$_{25}$]$_4$ (not shown) exhibited a low energy absorption maximum at around 450 nm, whereas TQPP-[*t*-Bu]$_2$-[OC$_{10}$H$_{21}$]$_4$ (Figure 1B) and TQPP-[*t*-Bu]$_2$-[OC$_{12}$H$_{25}$]$_4$ (not shown) showed a maximum at around 425 nm. The red shift in the absorption maximum of the sulfur-based TQPP-[*t*-Bu]$_2$-[SR]$_4$ (SC10 and SC10), in comparison to that of the oxygen-based TQPP-[*t*-Bu]$_2$-[OR]$_4$ (OC10 and OC12), may be attributed to the higher polarizability of the sulfur atom.

On the other hand, the absorption band around 330 nm did not change appreciably between oxygen- and sulfur-containing species. This band is at similar wavelength to that of the parent pyrene. As expected, as the concentration of TQPP-[*t*-Bu]$_2$-[XR]$_4$ was decreased, the absorbance at 425 nm (for OC10 and OC12) and 450 nm (for SC10 and SC12) decreased. At concentrations below 1 μM, however, no peak was observed for any of the TQPP-[*t*-Bu]$_2$-[XR]$_4$ molecules in this region. However, the band at around 330 nm was clearly identifiable even at 50 nM concentration.

The fluorescence excitation and emission spectra of OC10, OC12, SC10, and SC12 are given in Figure 2. Fluorescence maxima were observed at around 370 nm under excitation at 320 nm. No change in the fluorescence spectrum was observed when the excitation wavelength was changed to 350 nm. Unlike the absorption maximum, the fluorescence maximum was, in general, independent of whether sulfur or oxygen atoms were present. The fluorescence spectra of **1** and **2** were in the same range as that of pyrene, unlike other related derivatives reported earlier.[35,36,42,43] This clear resemblance was evident from the comparison of the excitation and emission spectra of TQPP-[*t*-Bu]$_2$-[XC$_{12}$H$_{25}$]$_4$ (C12 and C12) with that of pyrene,[18] as shown in Figure 3. Furthermore, when excited at 390 nm, the emission spectra of these TQPP molecules showed a similar behavior of excimer emission compared to pyrene, suggesting that the presence of additional conjugation did not influence the emission properties of the pyrene core, in contrast to other pyrene-based conjugated compounds;[36] for example, similar derivatives incorporating a crown ether[44] displayed longer wavelength emission than the present compounds.

With an increase in the concentration of the compounds **1** and **2**, another peak at around 430−470 nm appeared in the fluorescence spectra; this is attributed to excimer (excited-state dimer) formation. In parallel with our work, Gao et al. have recently reported the emission spectrum for pyrazine-containing acene-type molecules in the range of 430−550 nm, which is similar to reported values for other pyrene-based derivatives.[36,45] In order to confirm that the observed fluorescence was indeed due to excimer formation and not due to another fluorescence band (dual fluorescence), we also excited compounds **1** and **2** at 390 nm and observed an emission spectrum exactly equivalent to the excimer peak of pyrene (Figure 4), ruling out the possibility of a second fluorescent moiety emitting in the longer wavelength range (430−470 nm). The fluorescence spectrum at excitation wavelength 390 nm also further suggested that the longer wavelength absorption bands at around 430 nm (OC12 and OC10) and 450 nm (SC10 and SC12) correspond to excitation to nonfluorescent state.

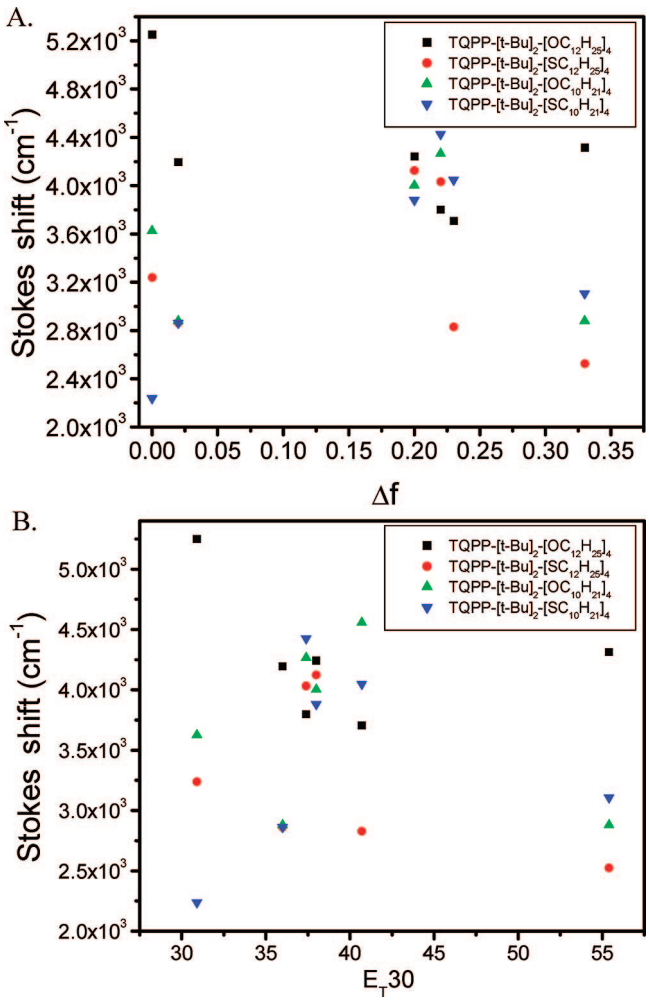

Figure 6. Stokes shift versus solvent polarity scale ((A) orientation polarizability, Δf; (B) E_T30 scale) for TQPP-[*t*-Bu]$_2$-[XR]$_4$.

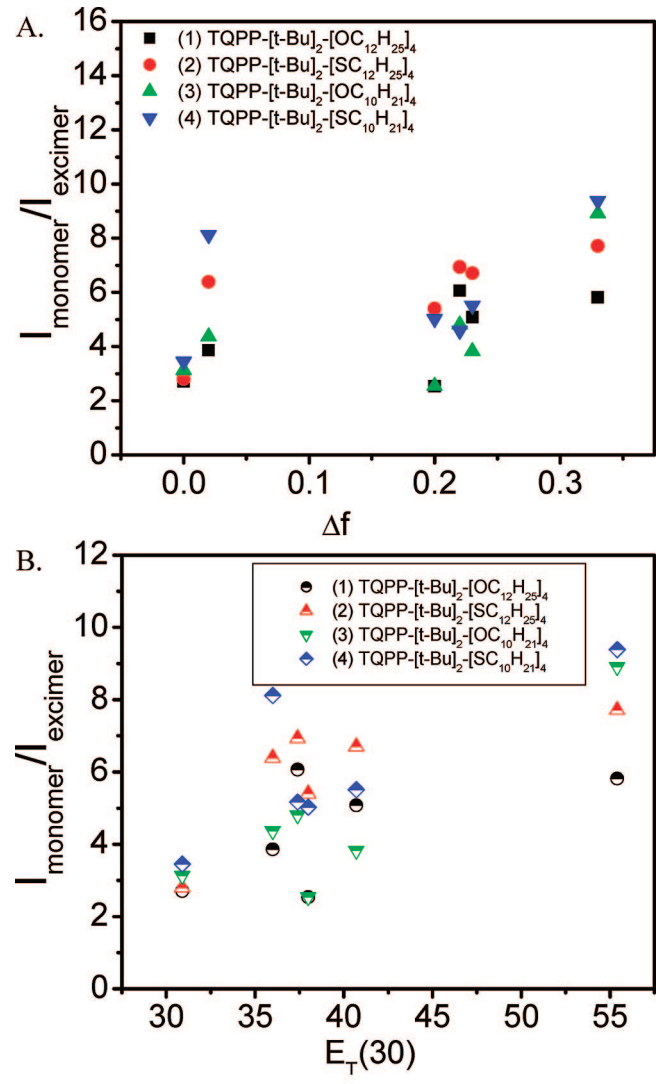

Figure 7. $I_{monomer}/I_{excimer}$ ratio for TQPP-[*t*-Bu]$_2$-[XR]$_4$ versus solvent polarity scale (E_T30 or Δf).

Excimer formation is further evident from Figure 2A where it can be seen that the peaks assigned to monomer and excimer emission both increase in intensity as the concentration is raised from 50 to 500 nM, whereas as the concentration is raised from 500 nM to 5 μM, the fluorescence intensity of the monomer peak decreases while that of the excimer peak increases dramatically, indicating that more monomers were participating in the excimer formation. For recording an excitation spectrum for monomer emission, the emission wavelength was fixed at 390 nm, whereas for excimer emission the emission wavelength was fixed at 450 nm. At 390 nm emission wavelength, the excitation spectrum at 50 nM concentration showed a maximum at around 310 nm, whereas at 450 nm emission wavelength, in addition to the 310 nm peak, another peak appeared at around 350−370 nm, with this band becoming more prominent at higher concentrations.

The absorption maxima at longer wavelength for SC12 in 1,2-dichlorobenzene, dichloromethane, and THF appeared at very similar wavelengths, whereas in cyclohexane the absorption maximum displayed a blue shift of around 25 nm. For OC12, the corresponding shift was only about 5−6 nm. However, the absorption maxima at shorter wavelength (around 320 nm) for SC12 in 1,2-dichlorobenzene, THF, and dichloromethane showed a solvent polarity dependent shift.

The excitation and emission spectra of SC12, SC10, OC12, and OC10 in various solvents are shown in Figure 5. The fluorescence spectra for all compounds clearly show an excimer emission peak at around 450 nm in cyclohexane, whereas in methanol none of the compounds shows any excimer peak. The excimer "emission" spectra in cyclohexane for OC12 and SC12 clearly show the vibronic bands associated with the excimer formation. This result indicates that, as the solvent polarity decreases from a polar (such as methanol) to nonpolar medium (such as cyclohexane), the aggregation behavior of TQPP molecules with extended chain length predominantly increases. The excimer emission spectra of the four compounds exhibit well-resolved fine structure in cyclohexane; this structure is successively less well-resolved as the solvent polarity is increased.

The absorption maxima, emission maxima, Stokes shifts (the difference between the maxima of the absorption and emission spectra[45]), and monomer/excimer intensity ratios of these compounds in various solvents are summarized in Table 1.

The Lippert−Mataga equation[45] shows that the solvent dependence of the Stokes shift for a compound depends on the change in the dipole moment of the fluorescence moiety upon excitation, the dielectric constant, and the refractive index of the solvents being used:[46,47]

$$\bar{\nu}_A - \bar{\nu}_F = \frac{2}{hc}\left(\frac{\varepsilon - 1}{2\varepsilon + 1} - \frac{n^2 - 1}{2n^2 + 1}\right)\frac{(\mu_E - \mu_G)^2}{a^3} + Constant$$

where $\bar{\nu}_A$ and $\bar{\nu}_F$ are the wavenumbers (cm^{-1}) of the absorbance and fluorescence maxima, respectively, with the difference between these two terms being the Stokes shift. h is Planck's constant, c is the speed of light in vacuum, a is the radius of the cavity in which the fluorophore resides, μ_E and μ_G are the dipole moments in the excited and ground states, respectively, and ε and n are the dielectric constant and the index of refraction of the solvents, respectively.[45]

The orientation polarizability (Δf) of the solvent, which is the result of both the drift velocity of electrons in the solvent and the dipole moment of the solvent, is defined as

$$\Delta f = \frac{\varepsilon - 1}{2\varepsilon + 1} - \frac{n^2 - 1}{2n^2 + 1}$$

The Lippert−Mataga plot can be obtained by plotting the Stokes shift versus Δf. In the case of charge transfer in a molecule, the gross solvent polarity indicator scale such as E_T30 is more applicable.[33,34]

Plots of Stokes shift versus the orientation polarizability (Δf) and E_T30 values of the solvents used are shown in Figure 6. As shown in the figure, the Stokes shift varies with both orientation polarizability (Δf) and solvent polarity (E_T30); however, this variation was not large and not systematic, giving the plots a scattered appearance. Particularly, large scattered values of Stokes shifts were obtained for solvents such as dioxane (for SC10 and SC12), 1,2-dichlorobenzene (for OC10 and OC12), and dichloromethane (for OC10 and SC10).

Pyrene and other synthesized pyrene-based molecules often exhibit a change in the ratio of the emission peak intensities of monomer over excimer when placed in solvents of different polarity. The fluorescence intensity ratio of monomer to excimer ($I_{monomer}/I_{excimer}$) is useful for solvatochromic studies using molecular probes such as pyrene.[48−52] In the present case, we also evaluated the fluorescence intensity ratio of monomer to excimer emission and found in most of the cases this ratio to be greater than 2 for the solvent under investigation (Figure 7 and Table 1). In the case of polar solvents such as methanol and 1,4-dioxane, this ratio was in the range 5−9. This high $I_{monomer}/I_{excimer}$ ratio in methanol/dioxane could be due to more monomer population compared to excimer formation. It is expected that aggregation of extended hydrocarbon chains is favorable in polar solvents such as methanol. However, the interaction among TQPP moieties through $\pi-\pi$ interaction of various molecules is likely to be less favorable, reducing excimer formation. In contrast, in nonpolar solvents, such as cyclohexane, extended hydrocarbon chains are soluble but TQPP cores are expected to come together to form $\pi-\pi$ interaction, increasing the chance of excimer formation and reducing the $I_{monomer}/I_{excimer}$ ratio.

The correlation of the monomer/excimer fluorescence intensity ($I_{monomer}/I_{excimer}$) with the E_T30 solvent polarity scale is found to be regular, as observed for other pyrene-based compounds,[18,42] for which studies using two types of solvents, such as protic and aprotic solvents, showed the correlation of $I_{monomer}/I_{excimer}$ versus E_T30 gave two intersecting straight lines (Mishra et al.[42]). However, in the present case, due to poor solubility of these compounds in many solvents of interest, a detailed analysis could not be carried out. For instance, for OC12 and SC12, we observed a large deviation of $I_{monomer}/I_{excimer}$ in methanol from a hypothetical regular change which could be due to the protic nature of this solvent.

The fluorescence lifetimes for monomer as well as excimer, fluorescence quantum yield, and radiative and nonradiative constants are also given in Table 2. The fluorescence lifetime studies for the four compounds show biexponential decay; the two decays can be attributed to that of the monomer and that of the excimer. The fluorescence lifetimes of all four monomers

TABLE 2: Monomer Lifetime, Excimer Lifetime, Fluorescence Quantum Yield, Radiative and Nonradiative Rate Constants of TQPP-[*t*-Bu]$_2$-[XR]$_4$ in Various Solvents at 25 °C

compound	solvents	$\tau_{monomer}$/ns	$\tau_{excimer}$/ns	ϕ_f	$k_r/(10^8\ s^{-1})$	$k_{nr}/(10^8\ s^{-1})$
TQPP-[*t*-Bu]$_2$-[OC$_{12}$H$_{25}$]$_4$	cyclohexane	2.59	11.50	0.79	3.03	0.83
	1,4-dioxane	3.29	15.80	0.87	2.64	0.40
	1,2-dichlorobenzene	1.91	12.08	0.69	3.63	1.61
	THF	3.65	11.27	0.09	0.25	2.49
	dichloromethane	2.27	11.52	0.15	0.67	3.73
	methanol	2.58	9.91	0.20	0.78	3.10
TQPP-[*t*-Bu]$_2$-[SC$_{12}$H$_{25}$]$_4$	cyclohexane	2.72	11.76	0.44	1.63	2.05
	1,4-dioxane	3.15	17.43	0.42	1.35	1.83
	1,2-dichlorobenzene	1.79	13.48	0.42	2.35	3.23
	THF	3.99	12.34	0.15	0.37	2.14
	dichloromethane	2.77	11.49	0.09	0.34	3.27
	methanol	3.49	10.77	0.18	0.51	2.35
TQPP-[*t*-Bu]$_2$-[OC$_{10}$H$_{21}$]$_4$	cyclohexane	3.41	12.20	0.88	2.58	0.35
	1,4-dioxane	5.02	19.10	0.67	1.32	0.67
	1,2-dichlorobenzene	2.28	13.32	0.17	0.75	3.64
	THF	4.17	12.83	0.02	0.04	2.35
	dichloromethane	3.35	12.06	0.47	1.40	1.58
	methanol	3.56	10.57	0.83	2.32	0.49
TQPP-[*t*-Bu]$_2$-[SC$_{10}$H$_{21}$]$_4$	cyclohexane	2.65	12.15	0.42	1.60	2.18
	1,4-dioxane	3.90	17.74	0.64	1.63	0.93
	1,2-dichlorobenzene	2.36	13.34	0.15	0.65	3.59
	THF	4.85	11.95	0.09	0.19	1.88
	dichloromethane	3.10	12.10	0.17	0.53	2.69
	methanol	3.42	10.45	0.46	1.35	1.58

in THF were longer than in any other solvent, whereas the fluorescence lifetime was shorter in 1,2-dichlorobenzene for the four compounds. The longer fluorescence lifetime of these compounds in THF and 1,4-dioxane can be explained due to the stabilization of the excited-state by the oxygen atom present in these solvents. On the other hand, the relatively short lifetime of the compounds in dichloromethane and 1,2-dichlorobenzene can be attributed to the fluorescence quenching effect by dichloromethane and 1,2-dichlorobenzene, as chlorinated compounds are known to increase the rates of nonradiative processes.[53,54]

The fluorescence quantum yield was determined as stated earlier using anthracene in ethanol as a standard reference. The fluorescence quantum yield was, in general, found to be small in THF for all TQPP-[*t*-Bu]$_2$-[XR]$_4$ molecules under investigation, whereas higher quantum yields were found in cyclohexane and dioxane.

The radiative rate constant was calculated by the equation[45]

$$k_r = \frac{\phi_f}{\tau_f}$$

where k_r is the radiative rate constant, ϕ_f is the fluorescence quantum yield, and τ_f is the fluorescence lifetime, and the nonradiative rate constant is evaluated as[45]

$$k_{nr} = \frac{1}{\tau_f} - k_f$$

The calculated radiative rate constants and nonradiative rate constants (Table 2) are of the order of 10^8 s^{-1} and are much greater than the corresponding values found for pyrene (approximately 10^6 s^{-1}).[18]

4. Conclusion

The synthesis of novel pyrene-based TQPP molecules and detailed studies of their photophysical properties have been described. These TQPP molecules possess four long chains of alkyloxy and alkylthio groups of various lengths. Concentration-dependent fluorescence measurements showed the formation of excimers even at nanomolar concentration. Although the solubility of these compounds was limited to a few organic solvents with variable polarities, detailed photophysical and spectroscopic characterization of these molecules in these solvents was carried out. Despite the structural differences between these TQPP molecules and pyrene itself, they showed similar fluorescence behavior to that of pyrene. However, the Stokes shift, monomer/excimer ratio, fluorescence lifetime, fluorescence quantum yield, and radiative and nonradiative rate constants were different from those reported for pyrene. Although the Stokes shift of these molecules showed a solvent polarity dependence, these results could not be correlated well with either Δf or E_T30 scales; however, correlation of the monomer/excimer intensity ratio with gross solvent polarity scales was reasonably regular. Compared to the pyrene molecule, such TQPP molecules showed much shorter fluorescence lifetimes, higher radiative rate constants, and greater tendencies to excimer formation.

Acknowledgment. This work was partially supported by the University Research Board (URB) of the American University of Beirut and the Lebanese National Council for Scientific Research (LNCSR). Acknowledgment is made to the Donors of the American Chemical Society Petroleum Research Fund (Grant No. 47343-B10) for partial support of this research. The authors are grateful for this support. We thank Dr. Steven Barlow, Prof. Makhlouf J. Haddadin, and Prof. Brigitte Wex for their valuable feedback.

References and Notes

(1) Tang, C. W.; VanSlyke, S. A. *Appl. Phys. Lett.* **1987**, *51*, 913.
(2) Palilis, L. C.; Murata, H.; Uchida, M.; Kafafi, Z. H. *Org. Electron.* **2003**, *4*, 113.
(3) Li, A. D. Q.; Li, L. S. *J. Phys. Chem. B* **2004**, *108*, 12842.
(4) Goes, M.; Verhoeven, J. W.; Hofstraat, H.; Brunner, K. *ChemPhysChem* **2003**, *4*, 349.
(5) Kraft, A.; Grimsdale, A. C.; Holmes, A. B. *Angew. Chem., Int. Ed.* **1998**, *37*, 403.
(6) Tang, C. W. *Appl. Phys. Lett.* **1986**, *48*, 183.
(7) Schmidt-Mende, L.; Fechtenkotter, A.; Müllen, K.; Moons, E.; Friend, R. H.; MacKenzie, J. D. *Science* **2001**, *293*, 1119.
(8) Garnier, F.; Hajlaoui, R.; Yassar, A.; Srivastava, P. *Science* **1994**, *265*, 1864.
(9) Dodabalapur, A.; Torsi, L.; Katz, H. E. *Science* **1995**, *268*, 270.
(10) Dimitrakopoulos, C. D.; Purushothaman, S.; Kymissis, J.; Callegari, A.; Shaw, J. M. *Science* **1999**, *283*, 822.
(11) Sirringhaus, H. *Adv. Mater.* **2005**, *17*, 2411.
(12) Kumar, S. *Chem. Soc. Rev.* **2006**, *35*, 83.
(13) Boden, N.; Bushby, R. J.; Clements, J.; Movaghar, B. *J. Mater. Chem.* **1999**, *9*, 2081.
(14) Van de Craats, A. M.; Warman, J. M.; Fechtenkötter, A.; Brand, J. D.; Harbison, M. A.; Müllen, K. *Adv. Mater.* **1999**, *11*, 1469.
(15) Sergeyev, S.; Pisula, W.; Geerts, Y. H. *Chem. Soc. Rev.* **2007**, *36*, 1902.
(16) Grozema, F. C.; Siebbeles, L. D. A. *Int. Rev. Phys. Chem.* **2008**, *27*, 87.
(17) Kollar, J.; Hrdlovic, P.; Chmela, S.; Sarakha, M.; Guyot, G. *J. Photochem. Photobiol., A* **2005**, *170*, 151.
(18) Karpovich, D. S.; Blanchard, G. J. *J. Phys. Chem. B* **1995**, *99*, 3951.
(19) Ren, K.; Serguievski, P.; Gu, H.; Grinevich, O.; Malpert, J. H.; Neckers, D. C. *Macromolecules* **2002**, *35*, 898.
(20) Toba, Y. *J. Photopolym. Sci. Technol.* **2003**, *16*, 115.
(21) Song, J. C.; Neckers, D. C. *ACS Symp. Ser.* **1995**, *598*, 472.
(22) Waris, R.; Rembert, M. A.; Sellers, D. M.; Acree, W. E., Jr.; Street, K. W., Jr.; Poole, C. F.; Shetty, P. H.; Fetzer, J. C. *Appl. Spectrosc.* **1988**, *42*, 1525.
(23) Waris, R.; Rembert, M. A.; Sellers, D. M.; Acree, W. E., Jr.; Street, K. W., Jr.; Fetzer, J. C. *Analyst* **1989**, *114*, 195.
(24) Waris, R.; Street, K. W., Jr.; Acree, W. E., Jr.; Fetzer, J. C. *Appl. Spectrosc.* **1989**, *43*, 845.
(25) Acree, W. E., Jr.; Tucker, S. A.; Zvaigzne, A. I.; Street, K. W., Jr.; Fetzer, J. C.; Grutzmacher, H. F. *Appl. Spectrosc.* **1990**, *44*, 477.
(26) Acree, W. E., Jr.; Tucker, S. A.; Cretella, L. E.; Zvaigzne, A. I.; Street, K. W., Jr.; Fetzer, J. C.; Nakasuji, K.; Murata, I. *Appl. Spectrosc.* **1990**, *44*, 951.
(27) Acree, W. E., Jr.; Zvaigzne, A. I.; Fetzer, J. C. *Appl. Spectrosc.* **1990**, *44*, 1193.
(28) Tucker, S. A.; Acree, W. E., Jr.; Street, K. W., Jr.; Fetzer, J. C. *Appl. Spectrosc.* **1989**, *43*, 162.
(29) Tucker, S. A.; Cretella, L. E.; Waris, R.; Street, K. W., Jr.; Acree, W. E., Jr.; Fetzer, J. C. *Appl. Spectrosc.* **1990**, *44*, 269.
(30) Tucker, S. A.; Acree, W. E., Jr.; Tanga, M. J. *Appl. Spectrosc.* **1991**, *45*, 57.
(31) Tucker, S. A.; Teng, I. L.; Acree, W. E., Jr.; Fetzer, J. C. *Appl. Spectrosc.* **1991**, *45*, 186.
(32) Powell, J. R.; Pandey, S.; Miller, B. J.; Acree, W. E., Jr.; Hansen, P. E.; Fetzer, J. C. *J. Lumin.* **1996**, *69*, 27.
(33) Reichardt, C. *Chem. Rev.* **1994**, *94*, 2319.
(34) Reichardt, C. *Solvents and Solvent Effects in Organic Chemistry*, 2nd ed.; VCH Verlagsgesellschaft, Weinheim, 1988.
(35) Shyamala, T.; Sankararaman, S.; Mishra, A. K. *Chem. Phys.* **2006**, *330*, 469.
(36) Gao, B.; Wang, M.; Cheng, Y.; Wang, L.; Jing, X.; Wang, F. *J. Am. Chem. Soc.* **2008**, *130*, 8297.
(37) Hu, J.; Zhang, D.; Jin, S.; Cheng, S. Z. D.; Harris, F. W. *Chem. Mater.* **2004**, *16*, 4912.
(38) Hu, J.; Zhang, D.; Harris, F. W. *J. Org. Chem.* **2005**, *70*, 707.
(39) Antonisse, M. M. G.; Snellink-Rueel, B. H. M.; Yigit, I.; Engbersen, J. F. J.; Reinhoudt, D. N. *J. Org. Chem.* **1997**, *62*, 9034.
(40) Kaafarani, B. R.; Lucas, L. A.; Wex, B.; Jabbour, G. E. *Tetrahedron Lett.* **2007**, *48*, 5995.
(41) Parker, C. A. *Photoluminescence of Solutions with Applications to Photochemistry and Analytical Chemistry*; Elsevier, Amsterdam, 1968.
(42) Subuddhi, U.; Haldar, S.; Sankararaman, S.; Mishra, A. K. *Photochem. Photobiol. Sci.* **2006**, *5*, 459.

(43) Venkataramana, G.; Sankararaman, S. *Org. Lett.* **2006**, *8*, 2739.
(44) Jradi, F. M.; Al-Sayah, M. H.; Kaafarani, B. R. *Tetrahedron Lett.* **2008**, *49*, 238.
(45) Lakowicz, J. R. *Principles of Fluorescence Spectroscopy*; Kluwer Academic, Plenum Publishers: New York, 1999.
(46) Lippert, E. *Z. Elektrochem.* **1957**, *61*, 962.
(47) Mataga, N.; Kaifu, Y.; Koizumi, M. *Bull. Chem. Soc.* **1956**, *29*, 465.
(48) Kalyanasundaram, K.; Thomas, J. K. *J. Am. Chem. Soc.* **1977**, *99*, 2039.
(49) Silva, M. A. d. R.; da Silva, D. C.; Machado, V. G.; Longhinotti, E.; Frescura, V. L. A. *J. Phys. Chem. A* **2002**, *106*, 8820.
(50) Winnik, F. M. *Chem. Rev.* **1993**, *93*, 587.
(51) Morawetz, H. *J. Polym. Sci., Part A: Polym. Chem.* **1999**, *37*, 1725.
(52) Somerharju, P. *Chem. Phys. Lipids* **2002**, *116*, 57.
(53) Motoyoshiya, J.; Fengqiang, Z.; Nishii, Y.; Aoyama, H. *Spectrochim. Acta, Part A* **2008**, *69A*, 167.
(54) Patra, D.; Mishra, A. K. *Appl. Spectrosc.* **2001**, *55*, 1725.

JP809830X